Science Advances

AAAS

advances.sciencemag.org/cgi/content/full/2/11/e1601478/DC1

Supplementary Materials for

Molecular structure of bottlebrush polymers in melts

Jarosław Paturej, Sergei S. Sheiko, Sergey Panyukov, Michael Rubinstein

Published 11 November 2016, *Sci. Adv.* **2**, e1601478 (2016)
DOI: 10.1126/sciadv.1601478

This PDF file includes:

Supplementary Materials

The size of a bottlebrush side chains in a melt

Figure S1 shows the dependence of the mean-square end-to-end distance $\langle R_{\text{sc}}^2 \rangle$ of side chains on the degree of polymerization N_{sc} obtained by molecular dynamics simulations of bottlebrush melts. The results of the computer simulations confirm theoretical predictions of Eq. (8), but indicate significant corrections due to small values of $N_{\text{sc}} \leq 32$ used in simulations. The mean-square end-to-end distance of a polymer chain $\langle R_{\text{sc}}^2 \rangle$ can be related to Flory's characteristic ratio $C_{N_{\text{sc}}}$ as follows $C_{N_{\text{sc}}} = \langle R_{\text{sc}}^2 \rangle / (N_{\text{sc}} \sigma^2) \approx C_{\infty}^{\text{sc}} / (1 + \tilde{N}_{\text{sc}} / N_{\text{sc}})$. For convenience we use σ instead of actual average bond length $l \approx 0.96\,\sigma$. Therefore $C_{N_{\text{sc}}}$ and C_{∞} are smaller than the actual Flory characteristic ratios by the factor $(l/\sigma)^2 \approx 0.92$. Simulation data are in reasonable agreement with this expression (dashed lines are for $N_{\text{bb}} = 100$) with fitting parameters $C_{\infty}^{\text{sc}} = 1.77$ and $\tilde{N}_{\text{sc}} = 1.01$ for $z = 1$ (red line) and $C_{\infty}^{\text{sc}} = 1.93$ and $\tilde{N}_{\text{sc}} = 1.15$ for $z = 2$ (black line), see table S1 for the list of C_{∞}^{sc} and $\tilde{N}_{\text{sc}}$ for different z and N_{bb}. The measured values of C_{∞}^{sc} for side chains are close to ≈ 2 which is typically observed for flexible chains (*54*). As expected, the grafted side chains are extended more than the corresponding linear chains (crosses $\times$ in fig. S1) in a melt (composed of the same number of monomers per chain). Direct comparison of the mean-square size of linear chains and bottlebrush side chains (both composed of 16 monomers) shows that the latter are larger by a factor of ≈ 1.12 for $z = 1$ and ≈ 1.22 for $z = 2$. The extension of side chains is attributed to the steric repulsion between monomers in the vicinity of attachment points, but their size still scales as $R_{\text{sc}} \propto N_{\text{sc}}^{1/2}$.

table S1. Summary of the adjustable parameters C_∞^{sc} and $\tilde{N}_{\text{sc}}$ describing the mean square size of side chains. The results represent the best fits of the mean square size of bottlebrush side chains by the expression $\langle R_{\text{sc}}^2 \rangle / (N_{\text{sc}} \sigma^2) = \frac{C_\infty^{\text{sc}}}{1+\tilde{N}_{\text{sc}}/N_{\text{sc}}}$ (see fig. S1).

N_{bb}	z	C_∞^{sc}	$\tilde{N}_{\text{sc}}$
10	2	1.83	1.02
20	2	1.89	1.09
50	2	1.92	1.13
100	1	1.77	1.01
100	2	1.93	1.15
150	2	1.94	1.15

table S2. Summary of system parameters for simulations of bottlebrush melts and linear chain melts. N_{bb} and N_{sc} correspond to the degree of polymerization of respectively backbone and side chains. The number of monomers per molecule is N, the number of molecules in a simulation box is M and the total number of monomers in a simulation domain is $\mathcal{N} = N \cdot M$. The side of corresponding cubic simulation box is a/σ. Symbols denote a particular bottlebrush melt in the figures throughout the manuscript.

N_{bb}	N_{sc}	z	N	M	$\mathcal{N}/10^3$	a/σ	symbol
10	0	0	10	500	5	18.05	×
20	0	0	20	400	8	21.11	×
50	0	0	50	250	12.5	24.49	×
100	0	0	100	200	20	28.66	×
150	0	0	150	200	30	32.80	×
10	1	2	30	500	15	26.03	▷
10	2	2	50	500	25	30.87	◁
10	3	2	70	500	35	34.45	⬠
10	4	2	90	500	45	37.55	▽
10	6	2	130	500	65	42.45	⬡
10	8	2	170	500	85	46.41	□
10	10	2	210	500	105	49.80	○
20	1	2	60	400	24	30.45	▷
20	2	2	100	400	40	36.10	◁
20	3	2	140	400	56	40.34	⬠
20	4	2	180	400	72	30.45	▽
20	6	2	260	400	104	49.66	⬡
20	8	2	340	400	136	54.23	□
20	10	2	420	400	168	58.25	○
50	10	1	550	200	110	50.58	●
50	1	2	150	250	37.5	35.33	▷
50	2	2	250	250	62.5	41.89	◁
50	3	2	350	250	87.5	46.87	⬠
50	4	2	450	250	112.5	50.96	▽
50	6	2	650	250	162.5	57.61	⬡
50	8	2	850	250	212.5	62.99	□
50	10	2	1050	250	262.5	67.59	○
50	10	4	2050	300	615	89.77	+
100	1	1	200	200	180	36.10	▶
100	2	1	300	200	180	41.33	◀
100	4	1	500	200	180	48.99	▼
100	8	1	900	200	180	59.60	■
100	10	1	1100	200	220	63.73	●

100	16	1	1700	200	340	73.68	
100	32	1	3300	100	330	72.95	
100	1	2	300	200	60	41.33	
100	2	2	500	200	100	48.99	
100	3	2	700	200	140	54.81	
100	4	2	900	200	180	59.60	
100	6	2	1300	200	260	67.38	
100	8	2	1700	200	340	73.68	
100	10	2	2100	200	420	79.06	
100	16	2	3300	100	330	72.95	
150	1	2	450	200	90	47.31	
150	2	2	750	200	150	56.09	
150	3	2	1050	200	210	62.75	
150	4	2	1350	200	270	68.23	
150	6	2	1950	200	390	77.12	
150	8	2	2550	200	510	84.34	
150	10	2	3150	200	630	90.49	

Persistence length of a bottlebrush in a melt

The decay of backbone bond orientational correlations $g(s)$ as functions of the number of backbone monomers s between two bonds for bottlebrushes with various degrees of polymerization N_{sc} of side chains is presented in fig. S2. The results of the computer simulations (symbols) have been fitted to the empirical bond orientational function (dashed lines) which is given by

$$g(s) = (1 - A)e^{-s/s_f} + Ae^{-s/s_p} + \varsigma s^{-3/2} \tanh\left[(s/s^*)^3\right] \tag{S1}$$

Fitting parameters A, s_f, s_p and ς are listed in table S3. The hyperbolic tangent function was introduced to eq. S1 in order to remove singularity of the power-law term $\propto s^{-3/2}$ at $s = 0$. In all fittings the power-law term was smoothly cut by setting the value of the parameter s^* to 3. The values of parameters A and s_f are almost independent of the side chain degree of polymerization N_{sc} for a given grafting density z. As displayed in Fig. 6 in the main text the number of monomers in a persistence segment s_p grows with N_{sc} as a power law: $s_p = 1.91N_{sc}^{0.53\pm0.04}$ for $z = 1$ and $s_p = 2.75N_{sc}^{0.48\pm0.03}$ for $z = 2$. The parameter ς is non-zero only for flexible bottlebrushes with persistent segment $s_p < 3.5$.

The Flory characteristic ratio C_∞^{bb} of bottlebrush backbones was calculated by the formula

$$C_\infty^{\text{bb}} = \lim_{N_{\text{bb}}\to\infty} \frac{\langle R^2(N_{\text{bb}})\rangle}{N_{\text{bb}}b^2} = 1 + \frac{2(1-A)}{e^{1/s_f}-1} + \frac{2A}{e^{1/s_p}-1} + \varsigma\tilde{C} \tag{S2}$$

with constant $\tilde{C} = 2\sum_{s=1}^{\infty} s^{-3/2}\tanh\left[(s/s^*)^3\right]$. The mean-square end-to-end distance $\langle R^2(N_{\text{bb}})\rangle$ in Eq. S2 is connected to the bond orientational correlation function $g(s)$ of eq. S1 by

$$\langle R^2(N_{\text{bb}})\rangle = N_{\text{bb}}b^2 + 2b^2\sum_{s=1}^{N_{\text{bb}}-1}(N_{\text{bb}}-s)g(s) \tag{S3}$$

The values of Flory characteristic ratio C_∞^{bb} calculated from Eq. S2 are identical to the values of C_∞^{bb} listed in table S4 which were obtained from the fitting procedure by utilizing Eq. 22.

The dependence of the number of monomers s_p per persistence segments obtained from the decay of bond orientational correlation function $g(s)$ given in eq. S1 is plotted in fig. S3 as a function of bottlebrush thickness $\langle R_{\text{sc}}^2\rangle^{1/2}$ for bottlebrushes with $z = 1$ and 2 side chains grafted per backbone monomer. The persistence segment s_p increases as a power law of the bottlebrush radius: $1.84(\langle R_{\text{sc}}^2\rangle^{1/2})^{0.94\pm0.05}$ for $z = 1$ and $2.06(\langle R_{\text{sc}}^2\rangle^{1/2})^{0.98\pm0.04}$ for $z = 2$, which is consistent with the predicted linear relationship $s_p\sigma \propto \langle R_{\text{sc}}^2\rangle^{1/2}$ (see Eq. 17, 19 and 20 in the main text).

table S3. Summary of the adjustable parameters A, s_f, s_p and ς describing the bond orientational correlation function. The results represent the best fits of the bond orientational correlation function given by the Eq. S1 (see fig. S2).

z	N_{bb}	A	s_f	s_p	ς
0	0	0.63	0.30	0.90	0.11
1	8	0.28	0.30	5.82	0
1	16	0.28	0.31	8.75	0
1	32	0.32	0.30	11.42	0
2	1	0.40	0.40	2.60	0.14
2	2	0.50	0.31	3.32	0.10
2	4	0.51	0.30	5.21	0
2	6	0.53	0.28	6.24	0
2	8	0.55	0.26	7.21	0
2	10	0.54	0.32	8.82	0
2	16	0.55	0.32	10.81	0

The size of a bottlebrush in a melt

table S4. Parameters C_∞^{bb} and $\tilde{s}$ describing the sizes of backbone sections. Flory characteristic ratio C_∞^{bb} and number of backbone monomers $\tilde{s}$ in a crossover segment defined by the expression relating the size of the bottlebrush backbone sections to the number of bonds s in these sections $\langle R^2(s)\rangle/(s\sigma^2) = \frac{C_\infty^{\text{bb}}}{1+\tilde{s}/s}$ (see Fig. 8).

N_{bb}	N_{sc}	z	C_∞^{bb}	s
150	0	0	1.70	1.05
50	10	1	4.38	6.90
100	16	1	5.63	8.71
100	32	1	8.01	12.52
150	1	2	2.91	3.53
150	2	2	3.87	5.06
150	4	2	5.48	7.04
150	10	2	9.59	12.22
100	16	2	12.13	16.51
50	10	4	170	222

In fig. S4 the values of the mean-square radius of gyration $\langle R^2_{g,\text{bb}}(N_{\text{bb}})\rangle$ of bottlebrush backbones are plotted as functions of the degree of polymerization of side chains N_{sc}. The mean-square radius of gyration of bottlebrush backbones $\langle R^2_{g,\text{bb}}(N_{\text{bb}})\rangle$ increases as a power law of side chain degree of polymerization $\langle R^2_{g,\text{bb}}(N_{\text{bb}})\rangle/N_{\text{bb}} \propto N_{\text{sc}}^{0.46\pm0.02}$. Both mean-square radius of gyration and end-to-end distance $\langle R^2\rangle$ are consistent with the predicted scaling $\langle R^2_{g,\text{bb}}(N_{\text{bb}})\rangle \propto \langle R^2(N_{\text{sc}})\rangle \propto N_{\text{bb}}N_{\text{sc}}^{1/2}$.

The distributions P of instantaneous values of the end-to-end distance R for linear and bottlebrush melts are presented in fig. S5. From fig. S5 one can observe that the position of the maximum in distributions of end-to-end distances R is shifted towards larger values with increasing values of N_{sc}. The inset of fig. S5 displays the distributions $\tilde{P}$ of the end-to-end distance $\langle R\rangle$ normalized by root-mean-square value $\langle R^2\rangle^{1/2}$. All data sets collapse on a nearly single curve and thus obey the same scaling corresponding to Gaussian chains. The distributions $\tilde{P}$ of rescaled radius of gyration $R_g/\langle R_g^2\rangle^{1/2}$ values (not shown) follow similar behaviour.

Bottlebrush melt preparation

The preparation of the initial configuration of concentrated bottlebrush melts is described in the Materials and Methods section of the main paper and schematically presented in fig. S6. This step was performed by contracting the simulation box from the large size corresponding to low concentration $0.03\ \sigma^{-3}$ to the target size with melt density $0.85\ \sigma^{-3}$. After reaching the desired melt density the simulations were continued up to about three relaxation times of each system. The variety of individual conformations of bottlebrushes in a melt state are displayed in fig. S7.

fig. S1. The size of side chains of a bottlebrush in a melt. The dependence of the mean-square end-to-end distance $\langle R_{\text{sc}}^2 \rangle$ of side chains normalized by $\sigma^2 N_{\text{sc}}$ on the side chain degree of polymerization N_{sc} for bottlebrushes with various backbone degrees of polymerization N_{bb}. The number of side chains grafted per backbone monomer is $z = 1$ and 2. All symbols are defined in Fig. 4B and table S2. Dashed lines represent best fits to the data for $N_{\text{bb}} = 100$ by the expression $\langle R_{\text{sc}}^2 \rangle / (N_{\text{sc}} \sigma^2) = \frac{C_{\infty}^{\text{sc}}}{1 + \tilde{N}_{\text{sc}}/N_{\text{sc}}}$ with $C_{\infty}^{\text{sc}} = 1.77$ and $\tilde{N}_{\text{sc}} = 1.01$ for $z = 1$ (red line) and $C_{\infty}^{\text{sc}} = 1.93$ and $\tilde{N}_{\text{sc}} = 1.15$ for $z = 2$ (black line) and for linear chains with $C_{\infty}^{\text{sc}} = 1.54$ and $\tilde{N}_{\text{sc}} = 0.74$ (purple line).

fig. S2. The bond angle correlation functions $g(s)$. The results obtained from simulations for bottlebrushes with various degree of polymerization of side chains N_{sc} and different number of side chains grafted per backbone monomer z: (A) $z = 1$ and (B) $z = 2$ (see table S2 and Fig. 4B for the definition of symbols). Dashed lines represent best fits to eq. S1 with fitting parameters presented in table S3.

fig. S3. Persistent segments of bottlebrushes in a melt. The number of monomers s_p in persistent segments obtained from the decay of the bond orientational correlation function $g(s)$ is plotted as a function of root mean square size of side chains $\langle R_{\text{sc}}^2 \rangle^{1/2}$ for bottlebrushes with $N_{\text{bb}} = 100$. The number of side chains grafted per backbone monomer is $z = 1$ and 2 as indicated (see table S2 and Fig. 4B for the definition of symbols). The lines represent the best power law fits close to the predicted linear dependencies (see SM text for details).

fig. S4. The size of backbones for bottlebrushes in a melt. The mean-square radius of gyration of bottlebrush backbone $\langle R^2_{g,\mathrm{bb}}(N_{\mathrm{bb}})\rangle$ normalized by its ideal mean-square size $N_{\mathrm{bb}}\sigma^2$ is plotted as a function of the degree of polymerization of side chains N_{sc} (see table S2 and Fig. 4B for the definition of symbols). The dashed line represents the best fit of the data with $N_{\mathrm{bb}} = 100$. Note that the mean-square radius of gyration for bottlebrushes with shorter backbones $N_{\mathrm{sc}} \leq 50$ does not follow the same scaling since these polymers are star-like.

fig. S5. Distribution of sizes for bottlebrushes in a melt. Probability distribution functions P of the end-to-end distance R for chains and bottlebrushes with $N_{\mathrm{bb}} = 150$ and various degrees of polymerization of side chain N_{sc}. As indicated in the legend, various colors are utilized to distinguish between the lines with different values of N_{sc}. The inset shows probability distribution functions $\tilde{P}$ of the end-to-end distance R normalized by its root-mean-square value $\langle R^2\rangle^{1/2}$. Dotted line represents normalized theoretical distribution of the end-to-end distances for Gaussian chains.

fig. S6. A scheme demonstrating sample preparation of a bottlebrush melt. Solid lines represent boundaries of the periodic simulation box.

fig. S7. Snapshots displaying conformations of bottlebrush molecules in a melt state. All bottlebrushes posses the same degree of polymerization of backbone ($N_{\mathrm{bb}} = 100$) and the same grafting density ($z = 2$) but different degree of polymerization of side chains: (A) $N_{\mathrm{sc}} = 1$, (B) $N_{\mathrm{sc}} = 4$, (C) $N_{\mathrm{sc}} = 10$, (D) $N_{\mathrm{sc}} = 16$. Middle column shows conformations with size comparable to the average radius of gyration $\approx R_g$ whereas left and right column correspond respectively to the cases with molecular sizes $< R_g$ (crumpled conformations) and $> R_g$ (extended conformations).

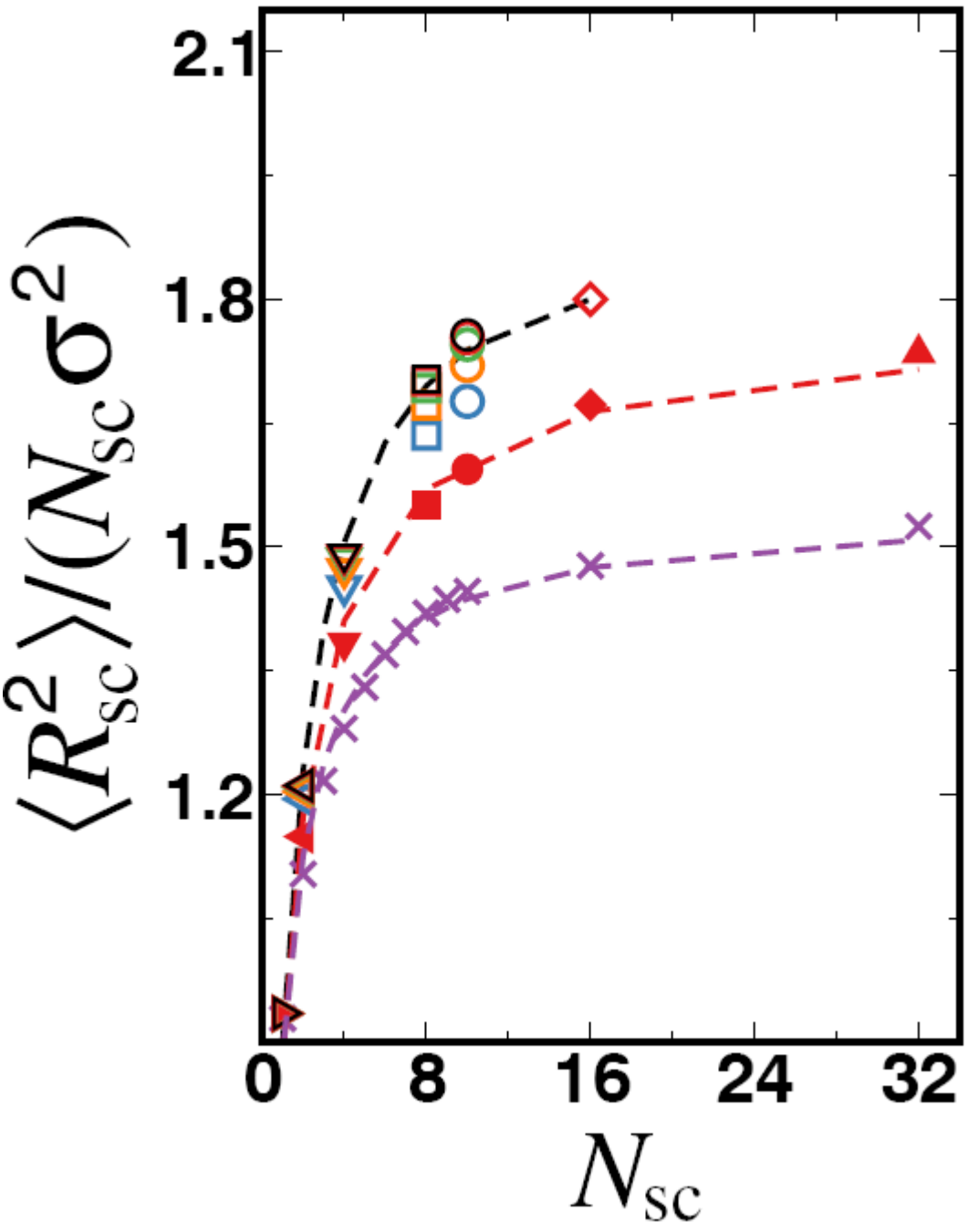

fig. S1.

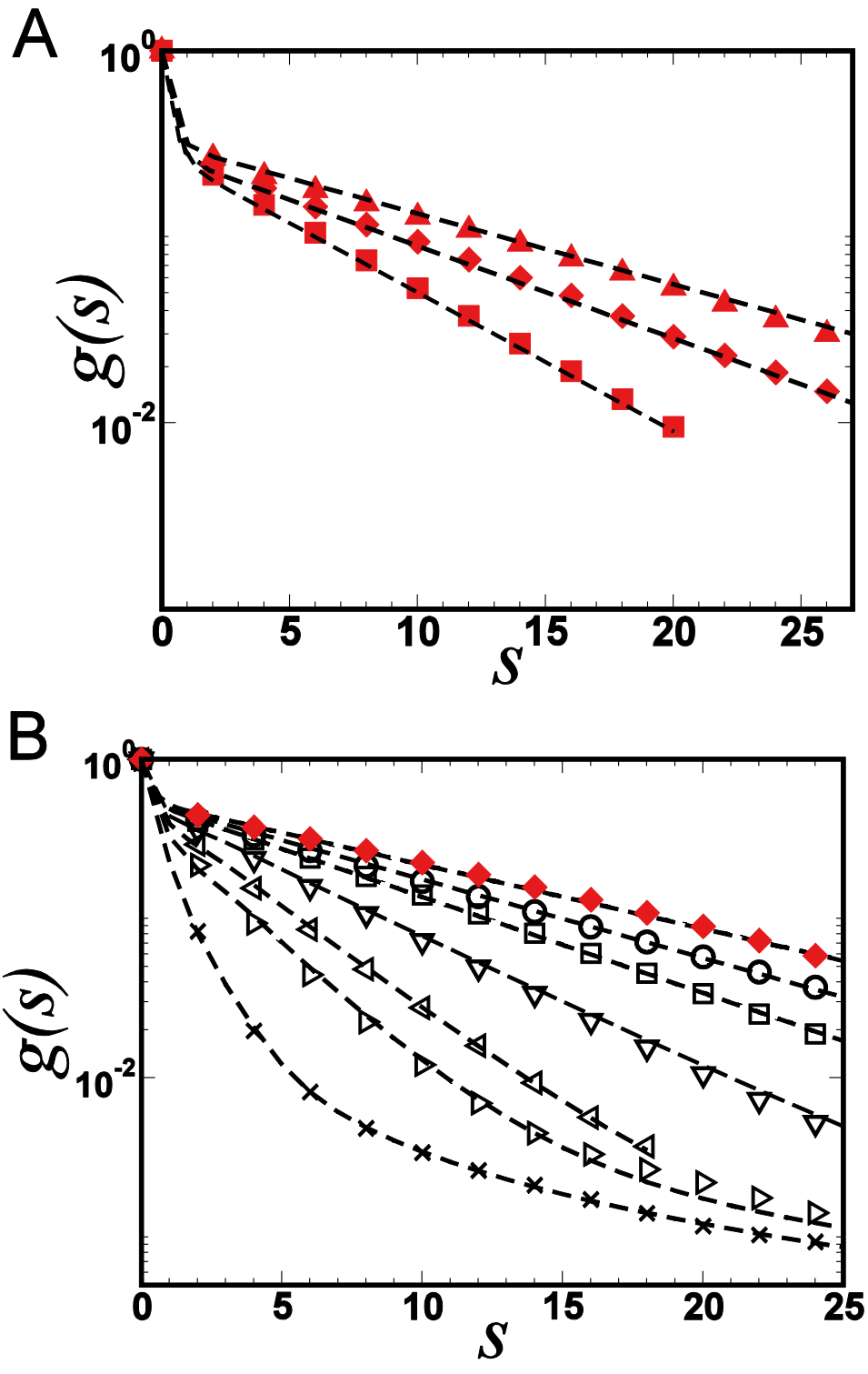

fig. S2.

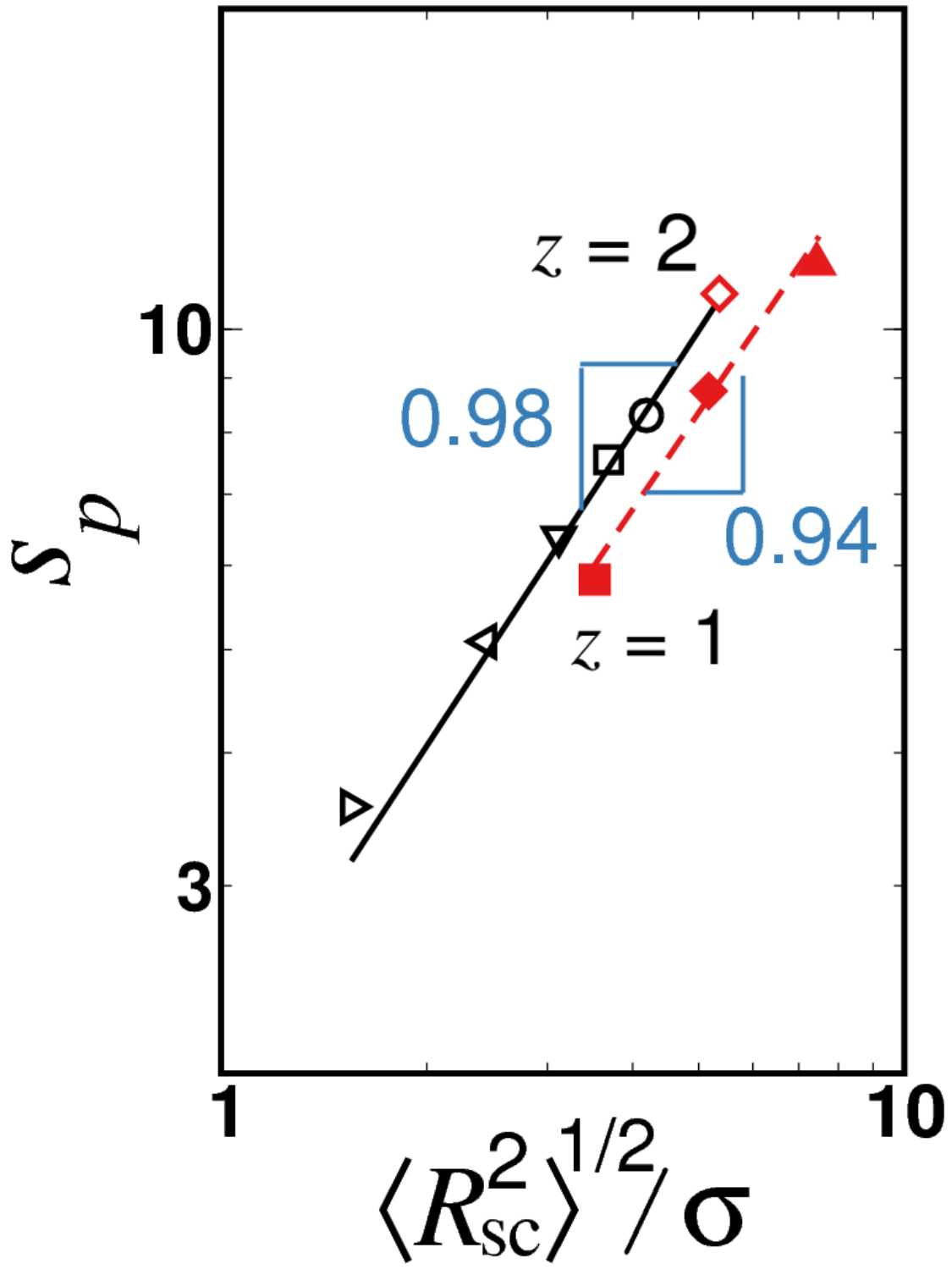

fig. S3.

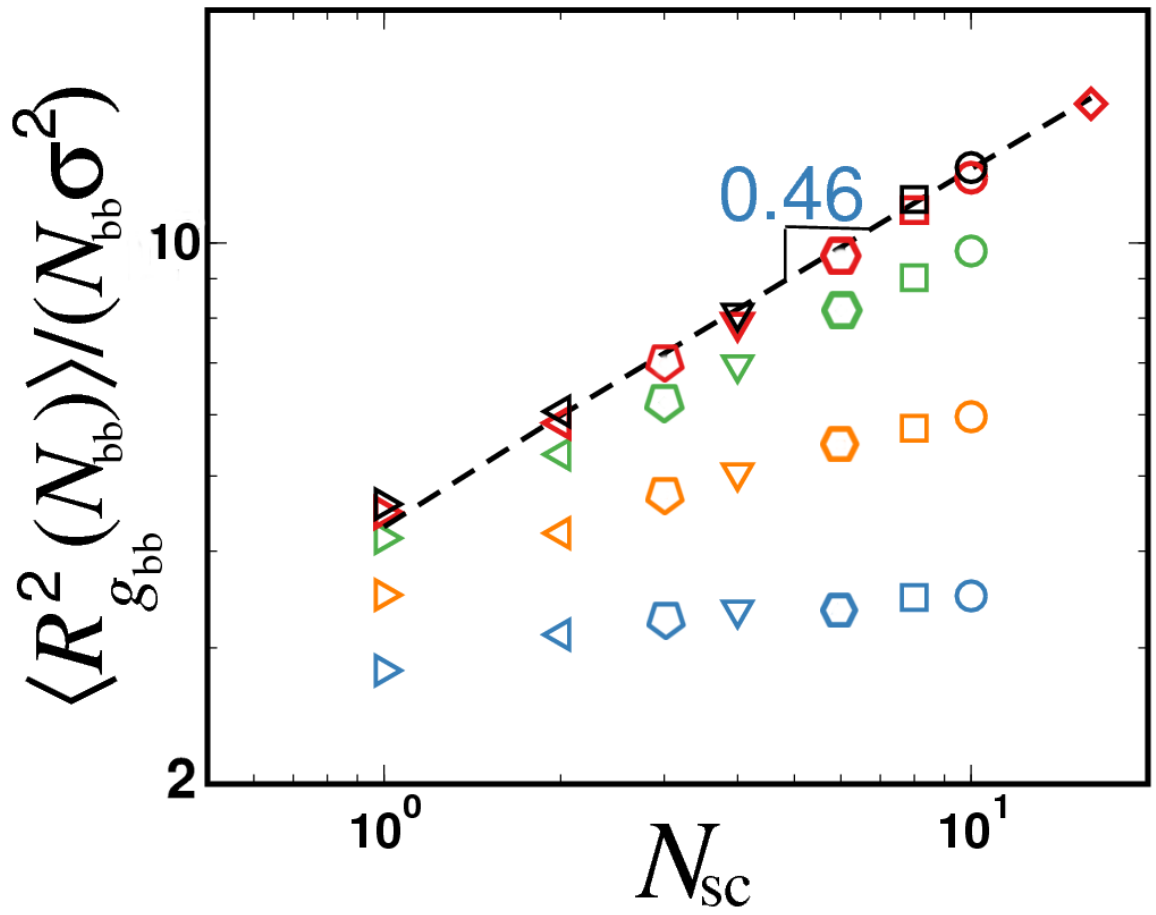

fig. S4.

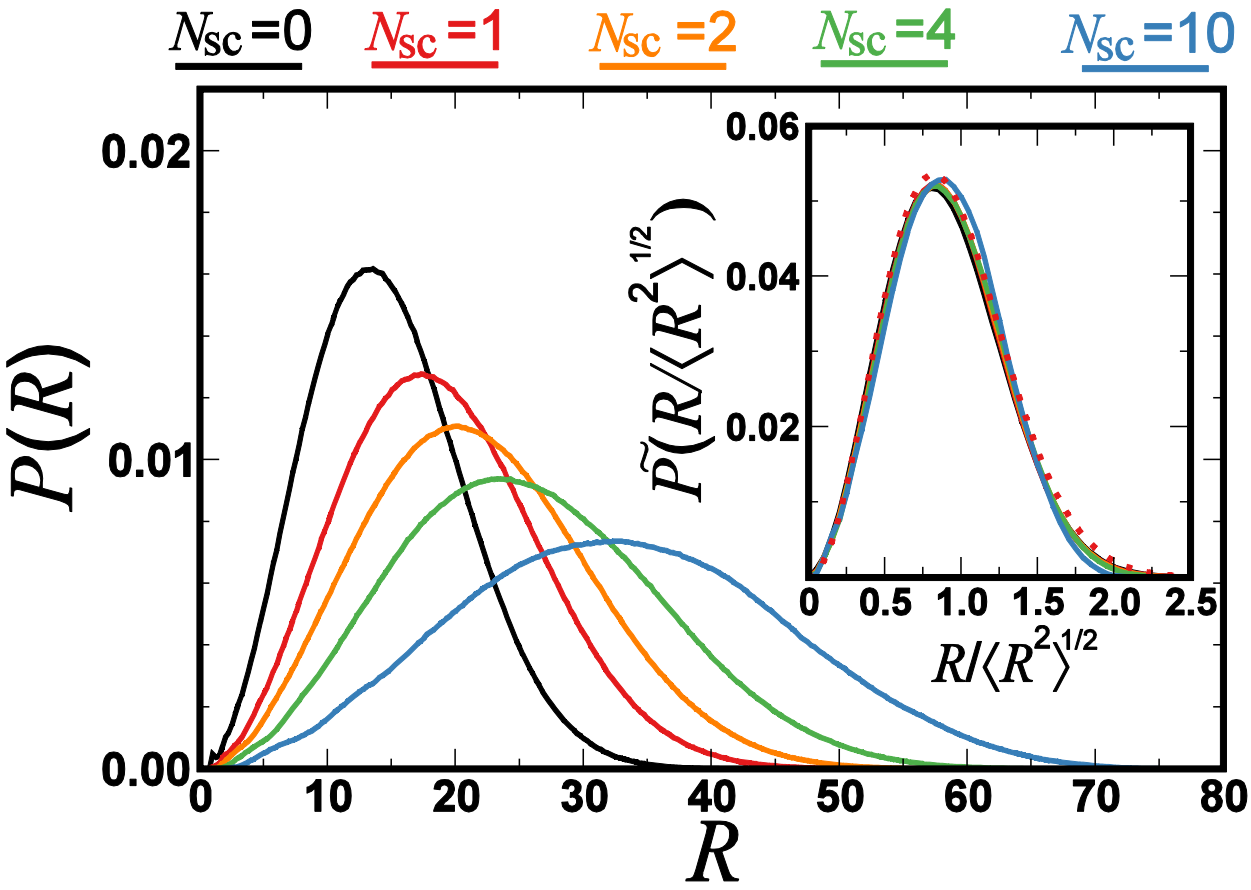
N_{sc} =0
N_{sc} =1
N_{sc} =2
N_{sc} =4
N_{sc} =10
P(R)
R
0.00
0.01
0.02
0
10
20
30
40
50
60
70
80
$\tilde{P}(R/\langle R^2\rangle^{1/2})$
$R/\langle R^2\rangle^{1/2}$
0.02
0.04
0.06
0
0.5
1.0
1.5
2.0
2.5

fig. S5.

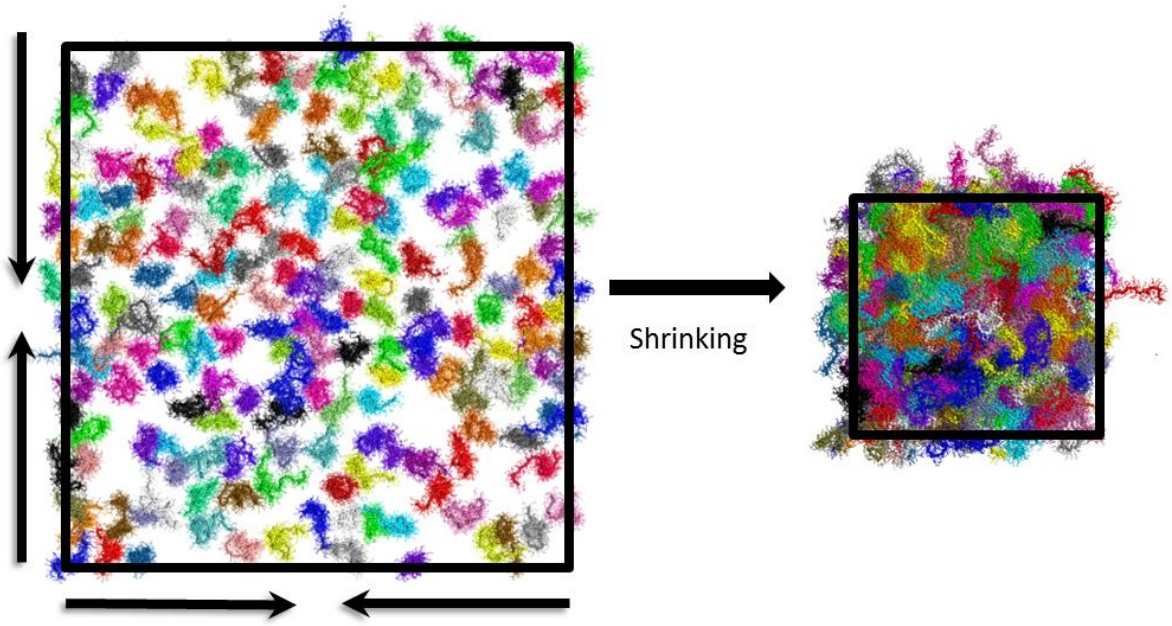

fig. S6.

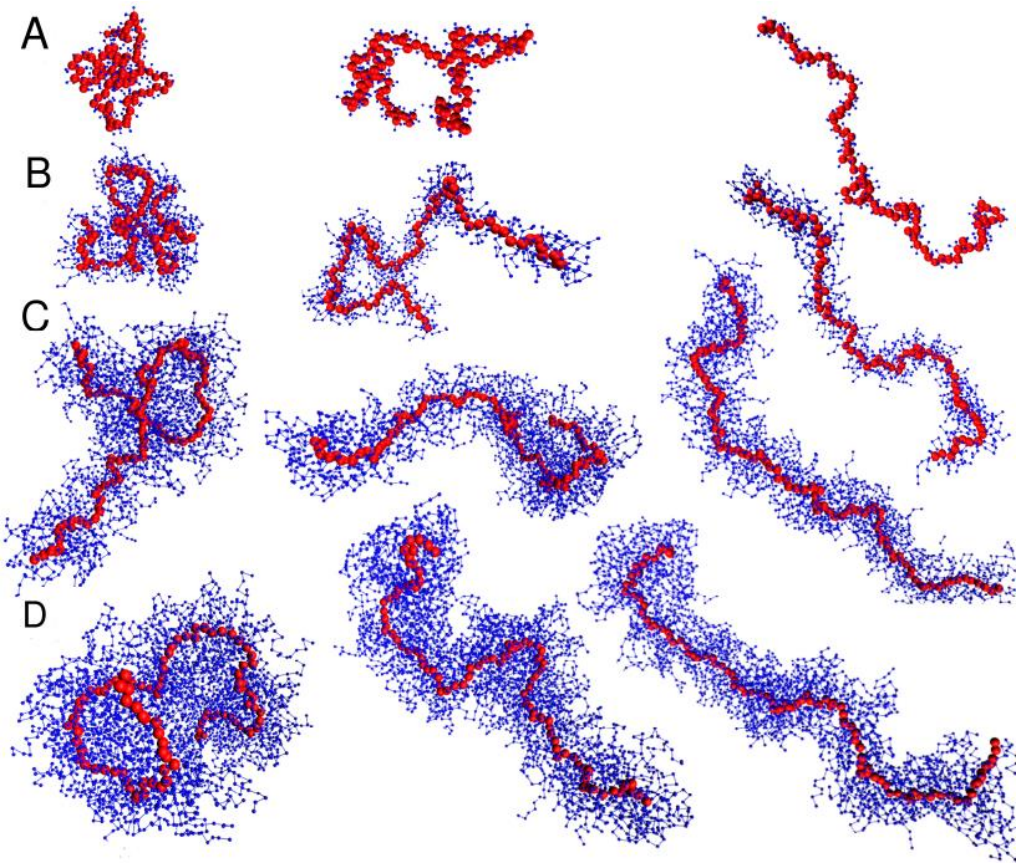

fig. S7.